Elsevier Editorial System(tm) for Soils and Foundations
Manuscript Draft

Manuscript Number: SANDF-D-16-00127R2

Title: Verification of a macro-element method in numerical simulation of the pore water pressure dissipation method -a case study on liquefaction countermeasure with vertical drains under embankment-

Article Type: Technical Note

Keywords: Macro-element method; Pore water pressure dissipation method; Soil-water coupled analysis; Liquefaction countermeasure

Corresponding Author: Mr. Toshihiro Nonaka, Master of Engineering

Corresponding Author's Institution: Nagoya University

First Author: Toshihiro Nonaka, Master of Engineering

Order of Authors: Toshihiro Nonaka, Master of Engineering; Shotaro Yamada, Doctor of Engineering; Toshihiro Noda, Doctor of Engineering

Abstract: In the simulation of the vertical drain method using a soil-water coupled finite elements analysis, a macro-element method has been often used as an approximate method to introduce the water absorption functions of drains into individual elements. In order to extend the function of this method, the authors modified the formula of the flow coefficient from soil to drains and introduced the discharge function of vertical drains to the method by treating the water pressure in the drains as an unknown and adding a continuity equation for the drains to the governing equations. The first attempt made it possible to divide a finite element mesh independently of the drain arrangement and the drain spacing, and the second attempt enabled that well resistance was automatically generated by a series of calculations depending on the given conditions. Furthermore, although the macro-element method has been applied to quasi-static problems in most cases, the authors applied the expanded one to dynamic problems by equipping it with the soil-water coupled finite deformation analysis code GEOASIA with the inertial term. In this paper, in order to verify the new macro-element method, in dynamic problem, the results of 2D approximate model using the new macro-element method was compared with those of 3D exact model where vertical drains were represented exactly by dividing finite element meshes finely, on a case of sand ground improved by the pore water pressure dissipation method under the embankment. The findings of this study are as follows: 1) 2D mesh-based analyses under plane strain condition using the new macro-element method can approximate 3D mesh-based analyses with fine mesh accurately in dynamic problem in terms of excess pore water pressure change and ground deformation; 2) the new macro-element method can adequately evaluate the influence of drain spacing on liquefaction countermeasure in a quantitative sense while using a single mesh; and 3) in the simulation of pore water pressure dissipation method, the new macro-element method improves calculation efficiency due to laborsaving in mesh-dividing and dramatically reducing in calculation time.

Manuscript_revision

Verification of a macro-element method in numerical simulation of the pore water pressure dissipation method -a case study on liquefaction countermeasure with vertical drains under embankment-

Toshihiro Nonaka[a], Shotaro Yamada[b], Toshihiro Noda[a]

[a]*Disaster Mitigation Research Center, Nagoya University, Nagoya, Japan*

[b]*Department of Civil Engineering, Nagoya University, Nagoya, Japan*

Abstract

In the simulation of the vertical drain method using a soil-water coupled finite elements analysis, a macro-element method has been often used as an approximate method to introduce the water absorption functions of drains into individual elements. In order to extend the function of this method, the authors modified the formula of the flow coefficient from soil to drains and introduced the discharge function of vertical drains to the method by treating the water pressure in the drains as an unknown and adding a continuity equation for the drains to the governing equations. The first attempt made it possible to divide a finite element mesh independently of the drain arrangement and the drain spacing, and the second attempt enabled that well resistance was automatically generated by a series of calculations depending on the given conditions. Furthermore, although the macro-element method has been applied to quasi-static problems in most cases, the authors applied the expanded one to dynamic problems by equipping it with the soil-water coupled finite deformation analysis code ***GEOASIA*** with the inertial term. In this paper, in order to verify the new macro-element method, in dynamic problem, the results of 2D approximate model using the new macro-element method was compared

with those of 3D exact model where vertical drains were represented exactly by dividing finite element meshes finely, on a case of sand ground improved by the pore water pressure dissipation method under the embankment. The findings of this study are as follows: 1) 2D mesh-based analyses under plane strain condition using the new macro-element method can approximate 3D mesh-based analyses with fine mesh accurately in dynamic problem in terms of excess pore water pressure change and ground deformation; 2) the new macro-element method can adequately evaluate the influence of drain spacing on liquefaction countermeasure in a quantitative sense while using a single mesh; and 3) in the simulation of pore water pressure dissipation method, the new macro-element method improves calculation efficiency due to laborsaving in mesh-dividing and dramatically reducing in calculation time.

Keywords: Macro-element method; Pore water pressure dissipation method; Soil-water coupled analysis; Liquefaction countermeasure

1. Introduction

In Japan, there have been significant concerns about the liquefaction damage caused by great earthquakes, after the damage of Tokyo Bay area in the 2011 Great East Japan Earthquake (Yasuda et al., 2012). The pore water pressure dissipation method (PWPDM) collects a lot of attention because this method is relatively inexpensive and superior in feasibility. However, the construction of liquefaction countermeasure with PWPDM has been hobbled by the lack of an effective analytical method of it.

The authors (Yamada et al., 2015) extended the functions of the macro-element, which is one of homogenization method, proposed by Sekiguchi et al. (1986), and designed a numerical-analysis technique that quantitatively evaluates the improvement effect of PWPDM by applying it to dynamic problems (Noda et al., 2015). The primary objective of this study is to verify this new method in dynamic problem on PWPDM.

One of the issues with numerical analysis of PWPDM is the enormous calculation cost because 3D analysis with fine mesh is required to represent a large number of vertical drains installed in ground. The authors have focused on the macro-element method as a means to resolve this issue. Since the macro-element method introduces the water absorption and discharge functions of drain into individual elements under 2D plane strain condition without using fine mesh, it is possible to improve calculation efficiency dramatically. Sekiguchi et al. (1986) attempted to express the accelerated consolidation associated with the vertical drain method using the macro-element method. Moreover, Sekiguchi et al. (1986) validated their proposed method through an observation conducted on a test embankment under which the soft ground was improved by the installation of sand drains. Although this method had been applied only to quasi-static problems, the authors applied it to dynamic problem by equipping it with the soil-water coupled analysis code ***GEOASIA*** (Noda et al., 2008) with the inertial term (Noda et al., 2015). And, the noteworthy features of the macro-element method proposed by the authors were that the division of finite element mesh could be specified independently of the drain arrangement and the drain spacing; and well resistance was automatically generated by a series of calculations depending on the given conditions.

In PWPDM, liquefaction during an earthquake is inhibited by suppressing the increase in pore water pressure by means of the installation of vertical drains. Instead of this, some degree of ground surface settlement due to compaction must be allowed for. Accordingly, in addition to the question of whether the method can be used to prevent liquefaction or not, it is important to be able to predict the degree of deformation that will occur as a result of ground compaction. This is the other issue with the numerical analysis of PWPDM. ***GEOASIA*** is capable of uniformly handling the following phenomena: 1) both compaction and liquefaction and 2) both the settlement due to compaction during an earthquake and the consolidation settlement after liquefaction. Therefore, it can also overcome this issue at the same time.

In the previous numerical-analysis approaches of PWPDM, drains were expressed as permeable boundaries (e.g., Tashiro et al., 2015) or expressed by increasing the permeability coefficient of the finite element (e.g., Papadimitriou et al., 2007). However, these methods require a fine mesh and an enormous calculation cost. On the contrary, homogenization methods enable us to avoid using a fine mesh. Poulos (1993), Omine et al. (1997, 1999), and Ng et al. (2015) considered homogenization methods for the ground improvement with columnar improvement method. Although quasi-static problems were targeted in these studies, verifications of these methods were conducted. Sato et al. (2005) and Ueda et al. (2015), among others, investigated homogenization methods for dynamic problem. These studies of dynamic problem did not match the progress of the quasi-static studies because the accuracy of one analysis was not verified, and the other was only a basic investigation employing linear analysis. Additionally, those studies only targeted SCP (sand compaction pile method), and PWPDM was not targeted.

Oka et al. (1992) and Kato et al. (1994) applied the macro-element method in a numerical analysis of PWPDM. They introduced the original macro-element method proposed by Sekiguchi et al. (1986), into LIQCA (Development group of liquefaction analysis code LIQCA, 2004) and examined the suppression of increase in excess pore water pressure (EPWP). However, the accuracy of this approximation has never been verified.

As previously mentioned, the authors have conducted numerical simulations of

PWPDM using the macro-element method with function extension (Noda et al., 2015). That study showed this method provided accurate approximations in the simulation of a single drain and the ground region where this drain was effective. Nevertheless, it remains to be shown that this method provides accurate approximations in the case of the simulation targeting a large scale and high heterogeneous problem where multiple drains and soil structures need to be treated. Moreover, in the previous study, only single verification was conducted for the case where the improvement effect was produced greatly. Therefore, more comprehensive verifications are required so that the macro-element method can earn higher credibility.

In this paper, the new macro-element method extended by the authors and introduced to the soil-water coupled analysis code ***GEOASIA*** was verified in a dynamic problem. A case of sand ground improved by PWPDM under the embankment was taken as an example. Specifically, the results of 2D mesh-based analysis under plane strain condition using the new macro-element method was compared to those of 3D mesh-based analysis in which vertical drains were represented exactly by dividing finite element meshes finely. Some analyses where drain spacing changed were conducted, and the cases were discussed not only where the improvement effect was produced greatly, but also where it was scarcely produced. And, as previously mentioned, the division of finite element mesh could be specified independently of the drain spacing, and the analyses with different drain spacing could be conducted while using a single mesh in the new macro-element method. To verify whether the numerical-analysis with this extension provided the appropriate results or not, it was confirmed whether the difference in improvement effect was properly produced or not in 2D mesh-based analysis. Finally, the reduction in analysis time using this new method was also discussed.

2. Outline of the application of the macro-element method to a soil–water finite

deformation analysis code with inertial terms

In this section, we will briefly summarize the macro-element method which is the target of verification and apply it to a soil-water finite deformation analysis code with inertial terms, based on Yamada et al. (2015) and Noda et al. (2015).

The soil–water finite-deformation analysis with inertial terms developed by the authors (Noda et al., 2008) employs a so-called $\boldsymbol{u}$–p formulation to obtain the nodal-displacement-velocity vector $\{\boldsymbol{v}^N\}$ and a representative pore water value u for each element by solving the space-discretized rate-type equation of motion and a soil–water coupled equation given by:

$$\mathrm{M}\{\ddot{\boldsymbol{v}}^N\} + \mathrm{K}\{\boldsymbol{v}^N\} - \mathrm{L}^{\mathrm{T}}\dot{u} = \{\dot{\boldsymbol{f}}\} \tag{1}$$

$$\frac{k}{g}\mathrm{L}\{\dot{\boldsymbol{v}}^N\} - \mathrm{L}\{\boldsymbol{v}^N\} = \sum_{i=1}^{m} \alpha_i (h - h_i)\, \rho_w g \tag{2}$$

where M is the mass matrix, K is the tangent stiffness matrix, L is the matrix for converting $\{\boldsymbol{v}^N\}$ to the elemental volume-change rate, $\{\dot{\boldsymbol{f}}\}$ is the material time derivative of the equivalent nodal force vector, h and h_i represent the total heads corresponding to the representative values of water pressure for a given element and for adjacent elements, respectively, k is the permeability coefficient for the ground, g is the magnitude of gravitational acceleration, α_i is the coefficient of pore water flow to adjacent elements, ρ_w is the density of water, and m is the number of boundary surfaces for each element. The first terms on the left-hand side of Eqs. (1) and (2) are the jerk term and the inertial term. The compressibility of water has been ignored for simplicity.

Next, the previously developed macro-element method with water absorption and discharge functions for vertical drains (Yamada et al., 2015) was applied to the analytical method above. First, we applied the following soil-to-drain pore water flow model to each element:

$$\dot{Q}_D = \kappa(u - u_D)\big(= \kappa(h - h_D)\rho_w g\big) \tag{3}$$

$$\kappa = \frac{8kV}{F(n)d_e^2\rho_w g} \tag{4}$$

$$F(n) = \frac{n^2}{n^2 - 1}\ln n - \frac{3n^2 - 1}{4n^2}, \quad n = \frac{d_e}{d_w} \tag{5}$$

E2

where $\dot{Q}_D$ is the soil-to-drain pore water flow rate, κ is the coefficient of pore water flow from the soil to the drain, u_D is the representative value for water pressure in the drain for each element, h and h_D are the total heads corresponding to u and u_D, respectively, and V is the current volume of each element. d_e and d_w represent the equivalent diameter and the diameter of the circular drain, respectively, and are treated as material constants. The derivation of the model is presented in Appendix A.

To incorporate the water-absorption function of vertical drains into each element, Eq. (3) is added to the right-hand side of Eq. (2), yielding the following expression:

$$\frac{k}{g}\mathrm{L}\{\dot{\boldsymbol{v}}^N\} - \mathrm{L}\{\boldsymbol{v}^N\} = \sum_{i=1}^{m} \alpha_i(h - h_i)\,\rho_w g + \kappa(h - h_D)\rho_w g \tag{6}$$

Eq. (6) is called the soil–water continuity equation and replaces Eq. (2) as the governing equation.

In the original formulation of the macro-element method (Sekiguchi et al. 1986), u_D or h_D was specified by the analyst/investigator as an analytical condition. However, the authors recently proposed treating this value as an unknown. The following continuity equation for the drain, which is virtually included in the macro element, is formulated to compensate as many equations as the increased unknowns under the assumption that the finite element mesh is divided approximately in the vertical direction from the top to the bottom of the improved region:

$$\kappa(h-h_D)\rho_w g=\sum_{j=1}^{2}\beta_j\left(h_D-h_{Dj}\right)\rho_w g \tag{7}$$

where, β_j is the coefficient of water flow through the virtual drain contained in each element and h_{Dj} is the total head of the drain contained in the elements above and below the macro element. For the sake of simplicity, it is assumed that water flow through the drain obeys the Darcy's law. Bearing in mind that the ratio of the cross-sectional area of the virtual drain to the area of the boundary surface between the elements connected above and below is $1/n^2$; β_j is given by the following equation:

$$\beta_j=\frac{k_w}{l^j}\frac{\boldsymbol{l}^j}{l^j}\cdot\boldsymbol{n}^j\frac{s^j}{n^2} \tag{8}$$

where each symbol is defined as illustrated in Fig. 1. k_w is the permeability coefficient for a circular drain and is treated as a material constant. The discharge function of the drains is incorporated into the macro-element method by treating the water pressure in the drain as an unknown while simultaneously adding Eq. (7) as a governing equation. The boundary conditions for Eq. (7) are handled in the same manner as the hydraulic boundary conditions for Eq. (2). The initial value of the water pressure in the drain is to be matched with the pore water pressure at the point when the macro-element method is applied, unless there is a specific reason for not doing the same.

Ultimately, Eqs. (1), (6), and (7) represent the governing equations when the macro-element method is applied. Solving these equations simultaneously yields $\{\boldsymbol{v}^N\}$, u, and u_D. As implied by the fact that Eq. (1) is used as it is, we assume that the effect of the vertical drain's presence on the element's stiffness and mass is negligible. In addition, we assume that the change in drain volume in Eqs. (6) and (7) is sufficiently small relative to the change in ground volume. E3

One noteworthy feature of the macro-element method introduced above is that the mesh division can be specified independently of drain arrangement and drain spacing (see Appendix A in detail). As reported in Yamada et al. (2015), the supplementary conditions for the original macro-element method proposed by Sekiguchi et al. (1986, 1988) are not necessary. For a detailed explanation of how the material constants d_e, d_w, and k_w are determined, see Yamada et al. (2015).

In addition, for analyses based on $\boldsymbol{u}$–p formulation, there is an upper limit on the permeability coefficient in terms of the time increment per step (Noda et al. 2008). Although this upper limit can hinder calculations when the drain is represented using a divided mesh, the drain permeability coefficient in the macro-element method is not subject to such constraints. For analyses based on the $\boldsymbol{u}$–p formulation, this point along with the improved calculation efficiency can be emphasized as merits of the macro-element method.

As mentioned above, we assumed that the rigidity of drains is negligible when deriving the macro-element method. Therefore, although the macro-element method is suitable for simulation of EPWPM using prefabricated artificial drains, additional efforts are required to simulate the gravel drain method. This is a limitation of the current macro-element method.

3. Verification of macro-element method under plane strain condition in dynamic problems

3.1 Analysis conditions

As shown in Fig. 2, a case of sand ground improved by PWPDM under an embankment was assumed as an analysis target. Grid drains with rectangular cross section (Research Association for DEPP Method, 2011) (width of 150 mm, thickness of 50 mm) with a constant drain spacing in the square pattern were installed in the soft sandy layer beneath the embankment. A drainage mat was spread between ground and embankment in order to avoid blocking drainage from drains.

Figure 3 shows the finite element mesh and the boundary conditions for the 3D mesh-based analysis in which vertical drains were represented exactly by dividing finite element meshes finely (exact model). For simplicity, a single row of drains perpendicular to the embankment was targeted for the analysis. Furthermore, symmetry was assumed, so the region that enclosed by the dashed lines in the plan view in Fig. 2 was used actually for the analysis. The elements representing the drains themselves were assigned the same material properties as the surrounding soil, so the stiffness of the drain was neglected. And permeable boundary was assigned between the elements representing drains and the elements adjacent to them horizontally in order to represent the water absorption and discharge functions of drain. The drainage mats were assumed to be under atmospheric pressure. The side of the element representing the drain was subjected to hydrostatic pressures corresponding to the depth from the top of drain. The side and bottom of the sand layer were assumed to be impermeable boundaries, and the ground surface was assumed to be atmospheric pressure. The nodes on the z-x plane were constrained not to move in the y direction, so that macroscopically, the plane strain condition could be satisfied. A periodic boundary was applied to the side boundary of the y-z plane, while a viscous boundary was applied to the x direction (Lysmer and Kuhleemeyer, 1969; Noda et al., 2009) and a fixed condition was applied to the y and z directions at the bottom boundary, when a seismic motion was inputted. In the exact model, it was necessary to use a fine mesh around the drains, so an extremely large number of elements in the mesh were unavoidable.

Figure 4 presents the finite element mesh and the boundary conditions for the 2D mesh-based analysis using the macro-element method (approximate model).

Macro-element method was applied to the elements in the region enclosed by the dashed lines. As with ground, boundary conditions of macro-element were assumed to be atmospheric pressure at the top and assumed to be impermeable at the bottom. In the macro-element method proposed by the authors (Yamada et al., 2015; Noda et al., 2015), the mesh division can be specified independently of drain arrangement and drain spacing, E1 so it is possible to conduct calculations for cases with different drain arrangement and spacing by using a common relatively coarse mesh.

As mentioned in Chapter 2, there was an upper limit for the permeability coefficient of element in terms of the time increment per step in analysis based on $\boldsymbol{u}$-p formulation (Noda et al., 2008). For example, when the time increment per step is 1/1000 s like during earthquake response analysis in this study, the upper limit for the permeability coefficient of element is about 0.4 cm/s. This value is quite low as the permeability coefficient of a drain. Accordingly, the drains of the exact model were represented not as elements with high permeability but as the permeable boundary. This means that drains of the exact model were assumed to have infinite permeability. Contrastingly, the drains of the approximate model were treated as ones with finite permeability by using the macro-element method. However, the results of analysis using macro-element method indicated that water pressures in the drains nearly equaled the hydrostatic distributions, so the difference in representation about the permeability of drain does not matter under the conditions especially in this study.

Embankment elements of 3 m high were added atop the horizontally layered sand ground in both models and consolidation calculations were continued until the models reached steady state. These embankment-ground systems were subjected to the input motion created by 0.5 doubling acceleration of seismic motion shown in Fig. 5 in the x direction through the viscous boundary, and consolidation was allowed to proceed until the EPWP had completely disappeared. The input motion is a simulated motion of an assumed Tokai-Tonankai-Nankai earthquake in Nagoya port, which was published by the Central Disaster Prevention Council, Japan in 2003. The maximum acceleration of this motion was approximately 180 gal, and the duration of the principal motion was quite long at approximately 100 s. Naturally, the calculations were exclusively performed on the single analysis code described above for both the quasi-static and the dynamic processes, from before the earthquake until the period following the end of the earthquake.

Table 1 shows the material constants and initial values for the ground and embankment, and Table 2 shows the material constants for the viscous boundary. The values listed in Table 1 are the same as used in a previous study (Noda et al., 2015), and they were determined based on experiments of a silica sand and are as same as the ones used in. The properties of the soil are as follows: mean diameter D_{50} = 0.25 mm, uniformity coefficient U_c = 1.79, internal friction angle ϕ = 26°. The initial degree of structure $1/R^*_0$ and the initial overconsolidation ratio $1/R_0$ were determined on the assumption that the soil was in relatively loose state (relative density D_r = 30 - 40 %). While $1/R^*_0$ and $1/R_0$ were given uniformly within the ground, the specific volume was distributed according to the overburden pressure (Noda et al., 2005). For a detailed explanation of these initial values, see Asaoka et al. (2002). Table 3 provides the material constants for the drains, i.e., macro-element. The macro-element method was produced on the assumption that the distribution of pore water pressure is in the axisymmetric condition around a circular drain. Meanwhile, the improved region associated with a single drain is generally not circular and the drain material is often distributed in a band such as grid drain targeted in this study. Therefore, the drain spacing d and the width a and the thickness b of the band shaped drain are needed to be converted into the parameters of equivalent diameter d_e and the drain diameter d_w, respectively. The following equations, which were obtained by equating the each cross-section area, were used to determine d_e and d_w in this study.

$$d_e = \frac{2}{\sqrt{\pi}}d \quad \text{: Square pattern} \tag{9}$$

$$d_w = 2\sqrt{\frac{ab}{\pi}} \quad \text{: Band shaped drain} \tag{10}$$

In this study, three cases were examined, unimproved, drain spacing d = 0.9 m and drain spacing d = 0.6 m, and the results of the exact model and those of approximate model were compared. These two kinds of drain spacing were selected from the range of construction results of PWPDM in Japan (0.4 m – 1.1 m) (Research Association for DEPP Method, 2011). In order to gain a direct grasp of only the improvement effect provided by the drains, the boundary between ground and embankment was assumed to be atmospheric pressure also in the unimproved cases. The same mesh was used for the calculations in the exact model for the unimproved case as in the case of d = 0.6 m. The same mesh was used for all cases in the approximate model. Table 4 shows the numbers of elements and degrees of freedom of both models (found from displacement of nodes, pore water pressure, water pressure in drains, and undetermined Lagrange constants related to periodic boundary conditions). Two meshes were used in the exact model, but there were no differences between them in the number of elements and degrees of freedom. Using the macro-element method allowed a large reduction in the number of elements and degrees of freedom.

3.2 Comparison of analysis results

Figure 6 shows the distributions of EPWP after the end of seismic motions (145 s). Aside from the unimproved case, the exact model shows distributions along three distinct vertical (x-z) planes (the unimproved case shows a uniform distribution in the y direction). In the unimproved case, the pore water pressure is high below the embankment. In both improved cases, however, the increase in water pressure below the embankment is suppressed by the discharge function of drains. In addition, the case with the smaller drain spacing has a greater effect of suppression of increase in water pressure. The exact model indicates great effect of suppression in the vicinity of the drains, even though this diminishes with distance from the drains. The distribution of EPWP of the approximate model in the case of d = 0.9 m is almost equivalent to that of exact model at 0.3 m away from drains, and that of approximate model in the case of d = 0.6 m is almost equivalent to that of exact model at 0.2 m away from drains (both distances correspond to the position about d/3 m away from drains). As shown above, the approximate model is able to express differences in suppression of water pressure due to changes in drain spacing while using a single mesh.

Figure 7 shows the relationships between time and EPWP ratio at the center of the improved region. Results at the initial depths of 1.5, 4.5, and 7.5 m are shown. For the exact model, EPWP ratio is the average value weighted by the volume for horizontally adjacent elements in the improved region assigned to the center drain. The unimproved case shows a high EPWP ratio until the end of the seismic motion. In contrast, in the two improved cases, even though EPWP ratio increases until the input acceleration reaches its highest value, subsequent to that, EPWP ratio decreases with the passage of time due to the effect of drains. Additionally, the case with smaller drain spacing shows sharp dissipation of water pressure. The approximate model evaluates the effect of drain spacing on the suppression of increase in water pressure quantitatively in all depths. EPWP ratio turns to negative values through the dissipation process. This is because the hydrostatic pressure of element decreases as the ground surface settles, which is caused by the fact that the boundary between ground and embankment is set to atmospheric pressure.

Figure 8 shows the EPWP distributions on a horizontal (*x*-*y*) plane in the exact model. The distribution is shown at the initial depth of 4.5 m near the center of the improved region. There is a radiating distribution of water pressures centered on the drain. In terms of the EPWP distribution along the radial direction from the center drain, the calculated values obtained in the exact model is compared with the assumed values in the approximate model in Fig. 9. In the exact model, the values for EPWP of elements are plotted at the initial depth of 4.5 m in the improved region assigned to the center drain. The EPWP distribution u (r, z, t) along the radial direction r assumed in the approximate model for time t and height z is described by the following equation:

$$u(r, z, t) = \frac{n^2}{n^2 - 1} \frac{f(r)}{F(n)} \left(\bar{u}(z, t) - u_w(z, t)\right) + u_w(z, t) \tag{11}$$

where, $f(r)$ is the first eigenfunction from the solution by Baron (1948) (see Appendix A). The water pressure values obtained in the calculations for the ground and the drain are substituted for mean water pressure in the equivalent diameter $\bar{u}$ (z, t) and the drain water pressure u_w (z, t) of eq. (3). Naturally, as shown in Fig. 8, the axial symmetry of the water pressure distribution around the drain predicted by the exact model is not perfect, but the results of both assumed values in the approximate model and calculated values obtained in the exact model are quite similar at all times. The appropriate assumptions of water pressure distribution for the approximate model bring about accurate predictions of deformation, as will be shown below.

The acceleration response and the deformation of ground are compared. Figures 10 to 13 show the relationships between time and horizontal acceleration, its Fourier spectrum, the relationships between time and horizontal displacements, and the relationships between time and settlement at the center of the boundary between ground and embankment, respectively. The results of the exact model are the values for the nodes in contact with drains. It was confirmed that nearly identical results were obtained at other nodes in the *y* direction. The approximate model provides responses nearly equivalent to those of the exact model in all figures. Closer the drain spacing, greater the suppression of increase in water pressure, and better the stiffness of ground is preserved. As a result, the notable amplification of the short-period components and the reduction in settlement occurred especially in the case of d = 0.6 m. The results of the approximate model reproduce features as described above. The responses of the exact and approximate model are nearly identical for the unimproved case, thereby suggesting that the mesh size has little influence over results.

Next, the deformations of the improved region will be compared. Figure 14 shows the deformations of the improved region and the embankment after consolidation. The horizontal displacement is relative to the center nodes of the bedrock (bottom of the analytical region). In the unimproved case, the ground loses shear stiffness and a large lateral flow occurs. On the other hand, in the two improved cases, since the decrease of the effective stress is inhibited and the shear resistance of the soil is kept, the lateral flow and the accompanying settlement are suppressing. Here as well, the approximate model accurately reproduces the predictions of the exact model for the overall deformation in the improved region.

The relationship between the mean effective stress and the specific volume can be compared in order to examine the behavior of elements in the ground. The elements to be compared are those at the initial depth of 4.5 m in the center of the improved region. The exact model shows the average value weighted by the volume for horizontally adjacent elements in the improved region assigned to the center drain. Figure 15 shows the behaviors of corresponding elements. The approximate model provides responses nearly equivalent to those of the exact model in all cases. The two improved cases show that the decrease of the effective stress became smaller during the earthquake as the drain spacing is reduced. Instead, there is greater compression due to compaction during the earthquake. These cases show lower compression due to consolidation after the earthquake, compared to that during the earthquake. The case of d = 0.6 m shows nearly zero compression after the earthquake. Thus, the suppression of increase in pore water pressure and the compaction of the ground that takes place in compensation for this, which are unique features of PWPDM, are accurately reproduced by the calculations of the approximate model.

3.3 Comparison of analysis times

Finally, we will compare the calculation times required for inputting the seismic motion by the exact and approximate model. The time increment for each step was 1/1000 s in both models, and iterative calculations were carried out at each step. 145,000 steps were required for calculations of 145 s seismic motion. Both models used the calculation environment shown in Table 5.

Table 6 shows the calculation times in both models. These times are the means for two improved cases. The approximate model required about 1/180 the time needed by the exact model. It is clear that the macro-element method, including the greatly saving labor of dividing mesh, provides a sizeable improvement in calculation efficiency.

4. Summary

The results of the 2D approximate model in plane strain condition using the new macro-element method were compared with those of the 3D exact model, in order to verify the new macro-element method introduced to the soil-water coupled finite deformation analysis code ***GEOASIA*** in numerical simulation of pore water pressure dissipation method. The main findings are as follows:

1. 2D mesh-based analyses under plane strain condition using the new macro-element method can approximate 3D mesh-based analyses with fine mesh accurately in dynamic problem in terms of excess pore water pressure change and ground deformation. The new macro-element method can also produce the extremely accurate approximation of the difference in the improvement effect according to drain spacing.
2. In the macro-element method extended by the authors, the division of finite element mesh can be specified independently of the drain arrangement and the drain spacing. As a result, this method can quantitatively approximate the differences in suppression of increase in water pressure due to drain spacing while using a single mesh. The extremely accurate approximation of the suppression effect in water pressure increase in this method enables even accurate quantitative predictions of the suppression effect in deformation.
3. The distribution of water pressure is assumed in the area surrounding the drain while supposing an axisymmetric unit cell model surrounding a single drain in the macro-element method. The excess pore water pressure distribution around the drain assumed for the approximate model adequately represents the results of analysis by the exact model. This appropriate assumption of water pressure distribution for the approximate model brings about accurate approximation results.
4. Application of the macro-element method improves calculation efficiency due to greatly laborsaving in mesh-dividing and dramatically reducing calculation times.

As the next step, the authors hope to validate the predictive ability of the macro-element method by comparing with model experiments or in-situ observations and propose an advanced procedure for performance-based design of PWPDM utilizing the method. E3

Acknowledgement

The authors express their deep gratitude to the Japan Society for the Promotion of Science for their support of this study with Grant-in-Aid for Scientific Research (A) 25249064.

Appendix A. Derivation of the flow coefficient κ from soil to drain of the macro-element method

In the macro element method, a representative value of the water pressure in the drain u_D is assigned at the center of the element in addition to the representative value of the pore water pressure u. The rate of pore water influx from soil to the drain $\dot{Q}_D$ is calculated based on the difference between these two water pressures, given by

$$\dot{Q}_D = \kappa(u - u_D)\big(= \kappa(h - h_D)\rho_w g\big) \tag{A1}$$

where h and h_D represent the total heads corresponding to u and u_D, respectively. κ is the coefficient of pore water flow from the soil to the drain and must be specified to appropriately represent the effects of the drain spacing and diameter.

First, we assumed an axisymmetric unit cell model surrounding a single drain is concerned. Using $r_w(= d_w/2)$ as the radius of a circular drain, $r_e(= d_e/2)$ as the radius of the model, r as the distance to the center axis, z as the height from the bottom, t as time, $f(r)$ as the first eigenfunction from the solution by Barron (1948), and $u_w(z, t)$ as the water pressure in the drain, the distribution of water pressure $u(r, z, t)$ in the drain E2

$(0 \le r < r_w)$ and in the area surrounding the drain $(r_w \le r \le r_e)$ can be approximated as follows:

$$u(r,z,t) = \begin{cases} u_w(z,t) & (0 \le r < r_w) \\ g(z,t)f(r) + u_w(z,t) & (r_w \le r < r_e) \end{cases} \quad \text{(A2)}$$ E2

$$f(r) = \ln\frac{r}{r_w} - \frac{r^2 - r_w^2}{2r_e^2} \quad \text{(A3)}$$

where, $g(z,t)$ is a function describing the change in water pressure in the drain with height.

Next, we use the following expression to define the mean water pressure $\bar{u}(z,t)$ for the effective collector area $(r \le r_e)$ at a height z is defined by the following equation.

$$\bar{u}(z,t) = \frac{2\pi \int_0^{r_e} u(r,z,t) r dr}{\pi r_e^2} \quad \text{(A4)}$$

Substituting Eqs. (A2) and (A3) into Eq. (A4), we obtain the following equation.

$$\bar{u}(z,t) = g(z,t)\frac{n^2 - 1}{n^2}F(n) + u_w(z,t) \quad \text{(A5)}$$

$$F(n) = \frac{n^2}{n^2 - 1}\ln n - \frac{3n^2 - 1}{4n^2},\ n = \frac{r_e}{r_w} \quad \text{(A6)}$$ E2

When Eqs. (A2) and (A3) are used to describe the water pressure distribution, the rate of pore water influx from the soil to the drain per dz, $\dot{Q}_D^*(z,t)$, can be expressed by the following equation:

$$\dot{Q}_D^*(z,t) = 2\pi r_w dz \frac{k}{\rho_w g}\frac{\partial u}{\partial r}\bigg|_{r=r_w} = \frac{2\pi k dz}{\rho_w g}\frac{r_e^2}{r_e^2 - r_w^2}g(z,t) \quad \text{(A7)}$$

where k is the permeability coefficient of the ground. By deleting $g(z,t)$ from Eqs. (A5) and (A7), $\dot{Q}_D^*$ can be re-expressed by the following equation, using $\bar{u}$ and u_w.

$$\dot{Q}_D^*(z,t) = \frac{2\pi k dz}{F(n)\rho_w g}\left(\bar{u}(z,t) - u_w(z,t)\right) \quad \text{(A8)}$$

In other words, the equation describes how much pore water flows into the drain per improved area $\pi r_e^2 dz$ per unit time. Next, we convert the rate of influx into the drain $\dot{Q}_D^*$ to a per-element basis $\dot{Q}_D$. We consider u and u_D in Eq. (A1) as corresponding to $\bar{u}$ and u_w in Eq. (A8), respectively. Defining V as the volume of one element, when the ratio of $\dot{Q}_D^*$ to $\dot{Q}_D$ is assumed to be the same as the ratio of $\pi r_e^2 dz$ to V, the flow coefficient κ in Eq. (A1) can be expressed as follows.

$$\kappa = \frac{8kV}{F(n)d_e^2\rho_w g} \tag{A9}$$

In finite deformation analysis, the element volume V is matched to the actual volume. In addition, we allow the permeability coefficient k of the ground to change with the ground's void ratio. Meanwhile, d_e and d_w are employed as material constants that always have the same value irrespective of element deformation.

Sekiguchi et al. (1986) specified the κ of the original macro-element method based on the assumption that mesh division width was matched to the drain spacing or an integral multiple. On the other hand, the κ derived here enables the mesh division width to be assigned independently of the drain arrangement and spacing because using the element volume V in eq. (A9).

References

Asaoka, A., Noda, T., Yamada, E., Kaneda, K. and Nakano, M. (2002): An elasto-plastic description of two distinct volume change mechanisms of soils, *Soils and Foundations*, **42**(5), 47-57.

Barron. (1948): Consolidation of fine-grained soil by drain wells, *Transactions of the American Society of Civil Engineers* **113**(1), 718-742

Central Disaster Prevention Council. (2003): Assessment of damage in Tonankai Nankai earthquake (in Japanese).

Development group of liquefaction analysis code LIQCA. (2004): Data of LIQCA2D04 (open to the public in 2004).

Kato, M., Oka, F., Yashima, A. and Tanaka, Y. (1994): Dissipation of excess pore water pressure by gravel drain and its analysis, *Soils and Foundations*, **42**(4), 39-44 (in Japanese).

Lysmer, J. and Kuhleemeyer, R.L. (1969): Finite dynamic model for infinite media. American Society of Civil Engineers, *Journal of the Engineering Mechanics Division*, **95**(4), 859–877.

Ng, K.S. and Tan, S.A. (2015): Simplified homogenization method in stone column designs, *Soils and Foundations*, **55**(1), 154-165.

Noda, T., Asaoka, A. and Yamada, S. (2005): Elasto-plastic behavior of naturally deposited clay during/after sampling, *Soils and Foundations*, **45**(1), pp 51-64.

Noda, T., Asaoka, A. and Nakano, M. (2008): Soil-water coupled finite deformation analysis based on a rate-type equation of motion incorporating the SYS Cam-clay model, *Soils and Foundations*, **45**(6), 771-790.

Noda, T., Takeuchi, H., Nakai, K. Asaoka, A. (2009): Co-seismic and post-seismic behavior of an alternately layered sand-clay ground and embankment system accompanied by soil disturbance, *Soils and Foundations*, **49**(5), 739-756.

Noda, T., Yamada, S., Nonaka, T. and Tashiro, M. (2015): Study on the pore water pressure dissipation method as a liquefaction countermeasure using soil-water coupled finite deformation analysis equipped with a macro element method, *Soils and Foundations*, **55**(5), 1130-1139.

Oka, F., Yashima, A., Kato, M. and Sekiguchi, K. (1992): A constitutive model for sand based on the non-linear kinematic hardening rule and its application, *Proc. of 10th*

WCEE, 2529-2534.

Omine, K. and Ohno, S. (1997): Deformation analysis of composite ground by homogenization method, *Proc. of the 14th International Conference on Soil Mechanics & Foundation Engineering*, 719-722.

Omine, K., Ochiai, H. and Bolton, M.D. (1999): Homogenization method for numerical analysis of improved ground with cement-treated soil columns, *Proc. of the International Conference on Dry Mix methods for Deep Soil Stabilization*, 161-168.

Papadimitriou, A., Moutsopoulou, M., Bouckovalas, G. and Brennan, A. (2007): Numerical investigation of liquefaction mitigation using gravel drains, *Proceedings of 4th Int. Conference on Earthquake Geotechnical Engineering*, Thessaloniki, paper No. 1548.

Poulos, H.G. (1993): Settlement prediction for bored pile groups, *Proc. of the 2nd Geotechnical Seminar on Deep Foundations on Bored and Auger Piles*, Ghent, 103–117.

Research Association for DEPP Method (2011): Technical data on dissipation of excess pore water pressure method (in Japanese).

Sato, Y., Maeda, K., Hayashi, K., Murata, Y. and Takahara, T. (2005): A study on overall properties of seismic response and investigation method of counter-measured ground against liquefaction, *Journal of the Society of Materials Science*, Japan, **54**(11), 1141-1146 (in Japanese).

Sekiguchi, H., Shibata, T., Fujimoto, A. and Yamaguchi, H. (1986): A macro-element approach to analyzing the plane strain behavior of soft foundation with vertical drains, *Proc. of the 31st symposium of the JGS*, 111-116 (in Japanese).

Sekiguchi, H., Shibata, T., Mimura, M. and Sumikura, K. (1988): Behaviour of the seawall and bridge abutment at the edge of an offshore airport fill, *Ann., Disas. Prev.*

Res. Inst., Kyoto Univ. **32**(B-2), 123-145.

Tashiro, S., Asanuma, T., Oono, Y. and Hayashi, K. (2015): Quantitative evaluation of drainage effect by the pore water pressure dissipation method in horizontal bedded ground during a large earthquake, *Journal of Japan Society of Civil Engineers* A1, **71**(4), 145-158 (in Japanese).

Ueda, K. and Murono, Y. (2015): Fundamental study of seismic response analysis of inhomogeneous ground by using homogenization method, *Journal of the Japan Society of Civil Engineers*, **71**(4), 557-567 (in Japanese).

Yamada, S., Noda, T., Tashiro, M., and Nguyen, S. H. (2015): Macro element method with water absorption and discharge functions for vertical drains, *Soils and Foundations*, **55**(5), 1114-1129.

Yasuda, S., Harada, K., Ishikawa, K., and Kanemaru, Y. (2012): Characteristics of liquefaction in Tokyo Bay area by the 2011 Great East Japan Earthquake, *Soils and Foundations*, **52**(5), 793-810.

Table 1

Material constants and initial values (Noda et al, 2010).

	Ground (Sand layer)	Embankment
Elasto-plastic parameters		
Critical state index M	1.00	1.35
NCL intercept N	1.98	1.71
Compression index $\tilde{\lambda}$	0.050	0.110
Swelling index $\tilde{\kappa}$	0.016	0.020
Poisson's ratio ν	0.3	0.3
Evolution parameters		
Ratio of $-D_v^p$ to $\lVert \boldsymbol{D}_s^p \rVert$ c_s	1.0	1.0
Degradation index of structure a	2.20	2.00
Degradation index of OC m	0.10	0.50
Rotational hardening index b_r	3.50	0.10
Limitation of rotational hardening m_b	0.70	0.40
Fundamental parameters		
Soil particle density ρ_s (g/cm^3)	2.65	2.67
Permeability index k (cm/s)	1.0×10^{-3}	1.0×10^{-4}
Initial conditions		
Coefficient of lateral pressure K_0	0.6	0.6
Specific volume v_0	2.04 - 2.20	1.65 - 1.68
Degree of structure $1/R_0^*$	4.0	1.1
Overconsolidation ratio $1/R_0$	1.2	42.5
Degree of anisotropy ζ_0	0.0	0.0

Table 2

Material constants of viscous boundary.

Bedrock density ρ (g/cm^3)	2.00
S-wave velocity in bedrock V_s (m/s)	150.0

Table 3

Material constants of macro-element method.

Drain spacing d (m)	0.9	0.6
Equivalent diameter d_e (m)	1.02	0.68
Diameter of circular drain d_w (m)	0.10	0.10
Permeability coefficient of circular drain k_w (cm/s)	7.0×10^2	7.0×10^2

Table 4

Number of finite element mesh and degree of freedom.

	Number of finite element mesh	Degree of freedom
Exact model	10440	50529
Approximate model	635	2223

Table 5

Computing environment.

Central Processing Unit	Intel(R) Core(TM) i7-3970X 3.50 GHz
Memory	16.0 GB
Operating System	Windows 7 Professional

Table 6

Calculation time for an earthquake analysis (145sec).

Exact model	1697640 sec (19.6 day)
Approximate model	9630 sec (0.1 day)

Figure_revision

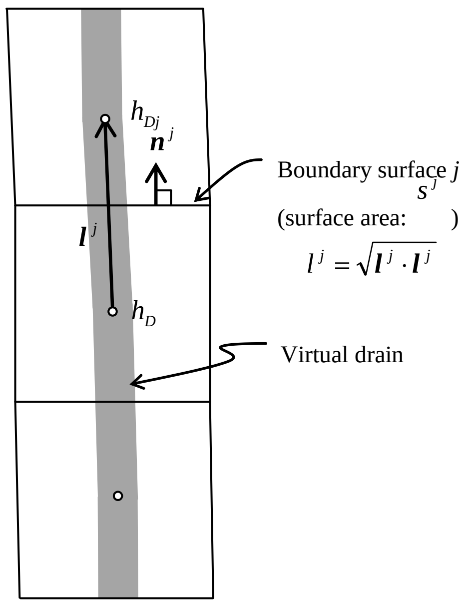

Fig. 1. Virtual drain contained in mesh.

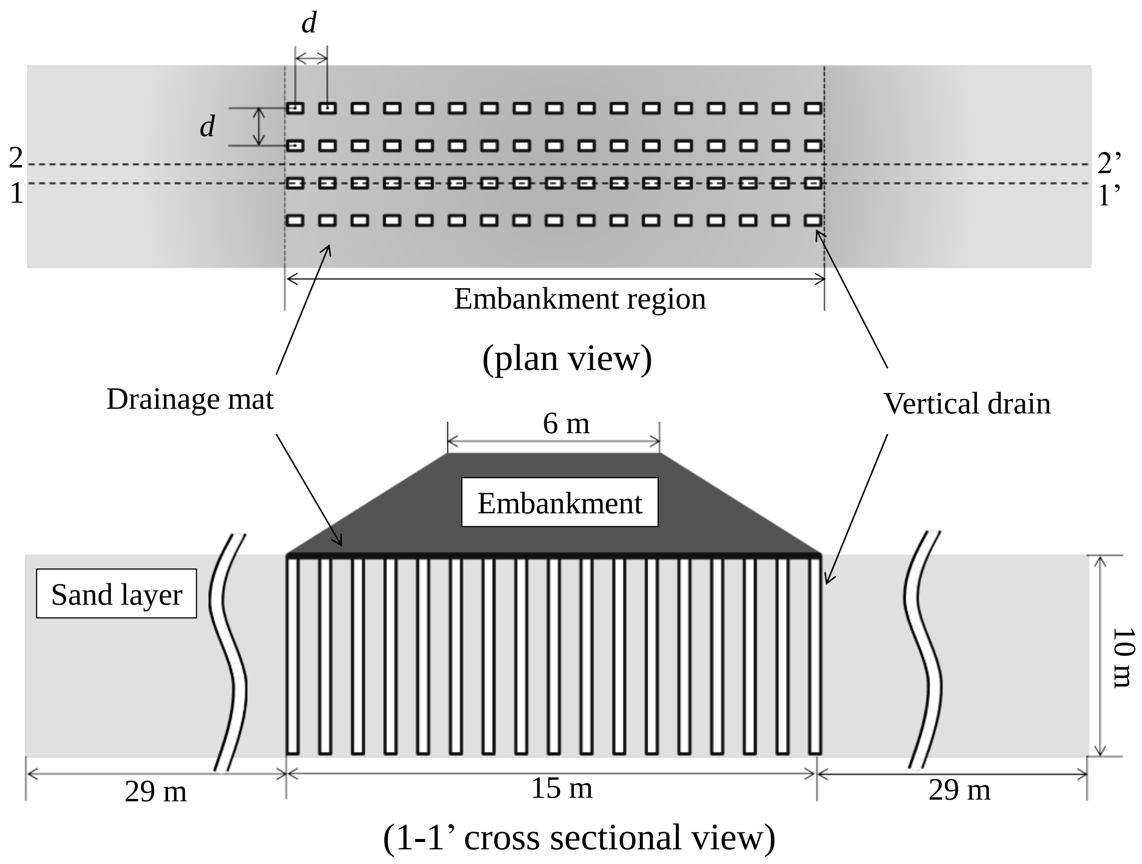

Fig. 2. Outline of analytical model.

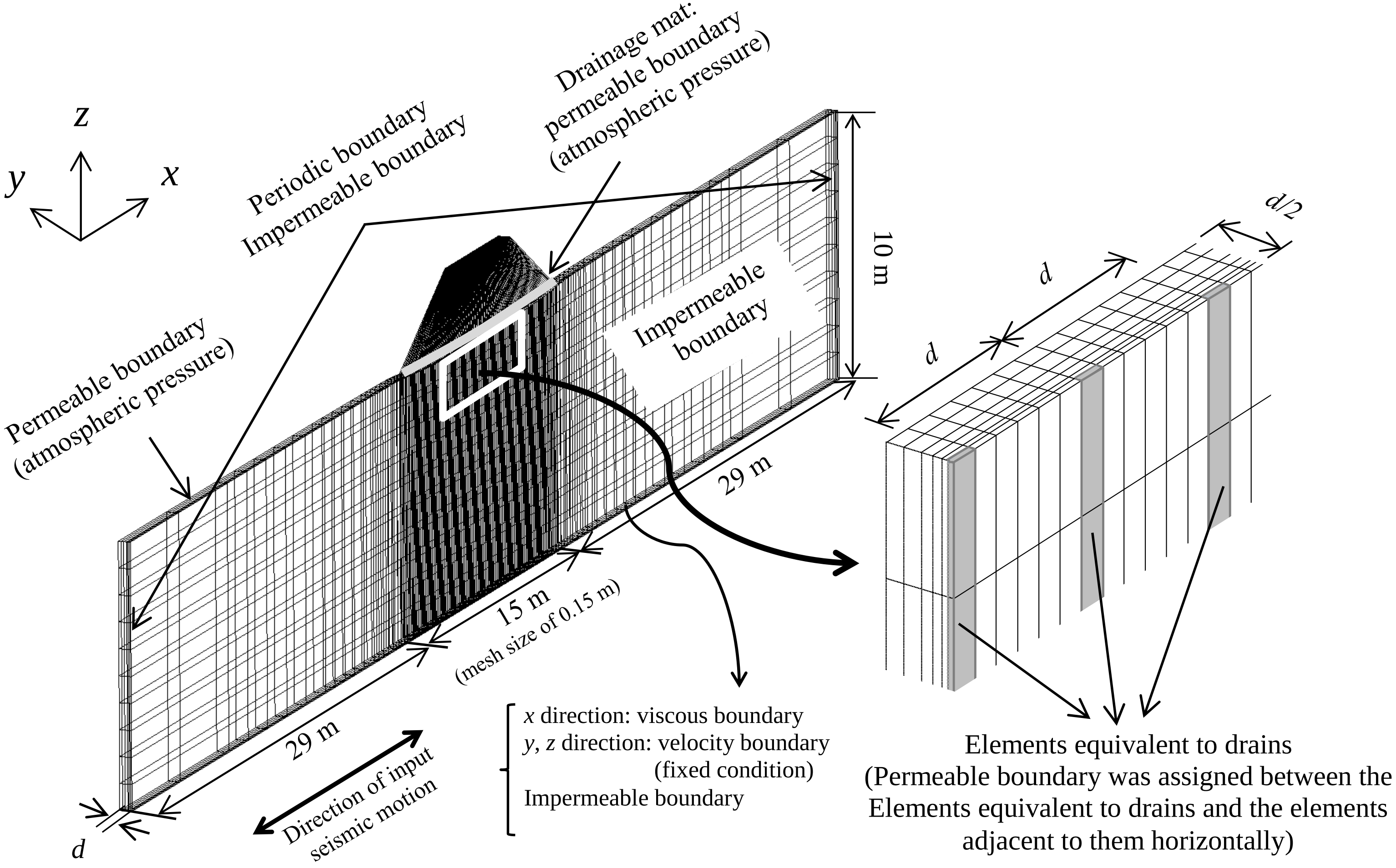

Fig. 3. Finite element mesh and boundary conditions (exact model).

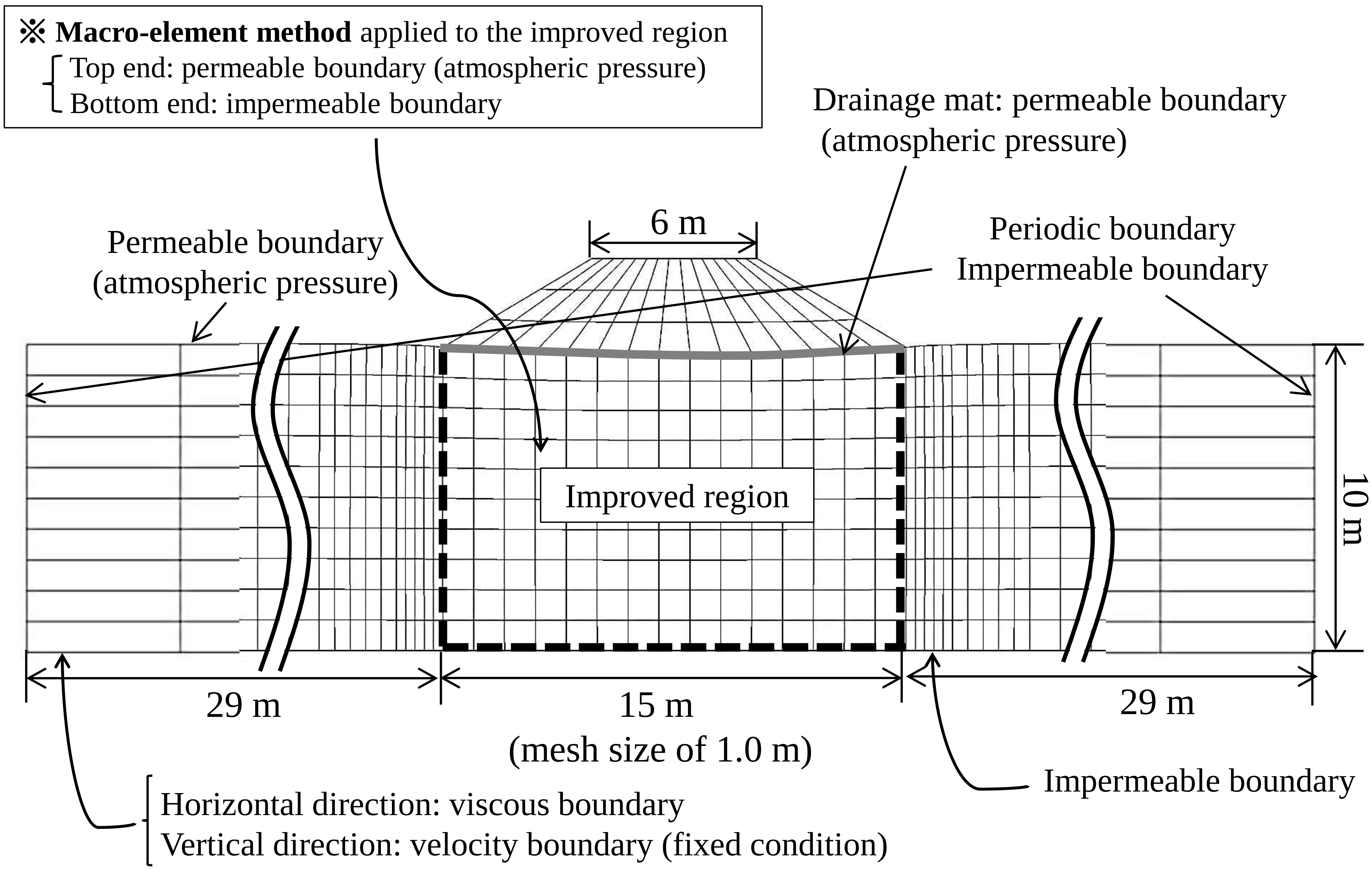

Fig. 4. Finite element mesh and boundary conditions (approximate model).

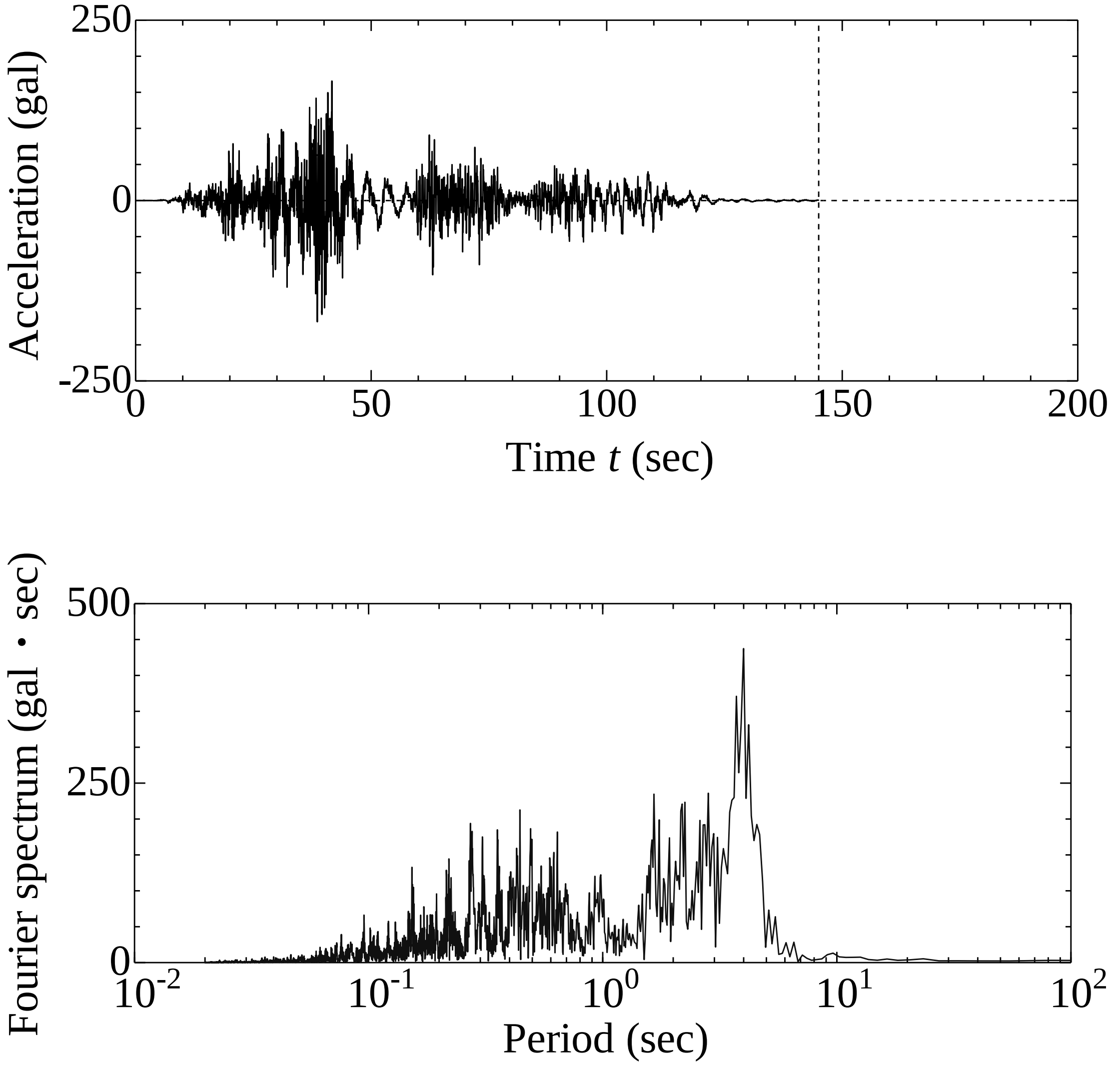

Fig. 5. Input seismic motion.

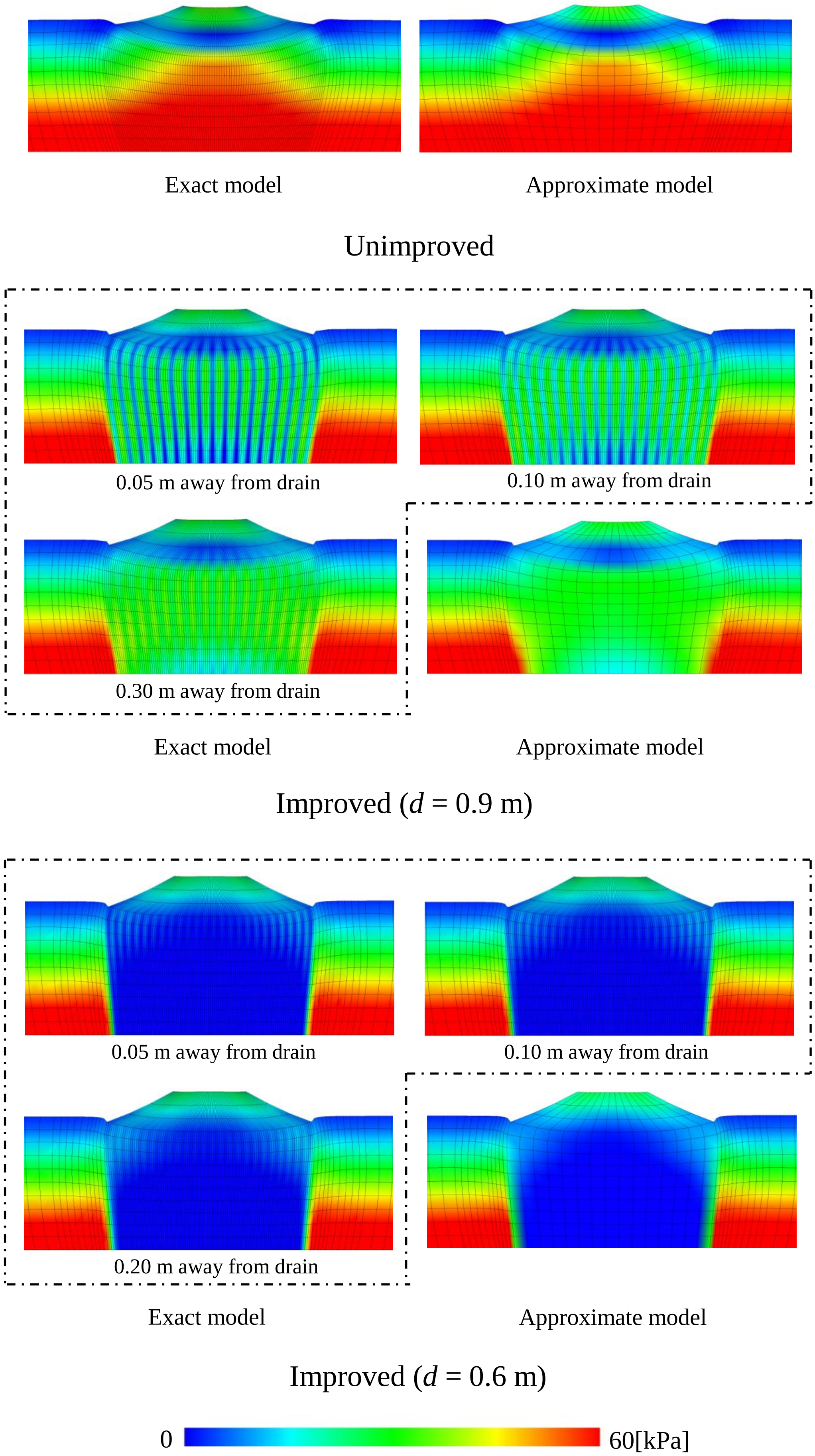

Fig. 6. Distributions of EPWP (*x*-*z* cross section, 145 s).

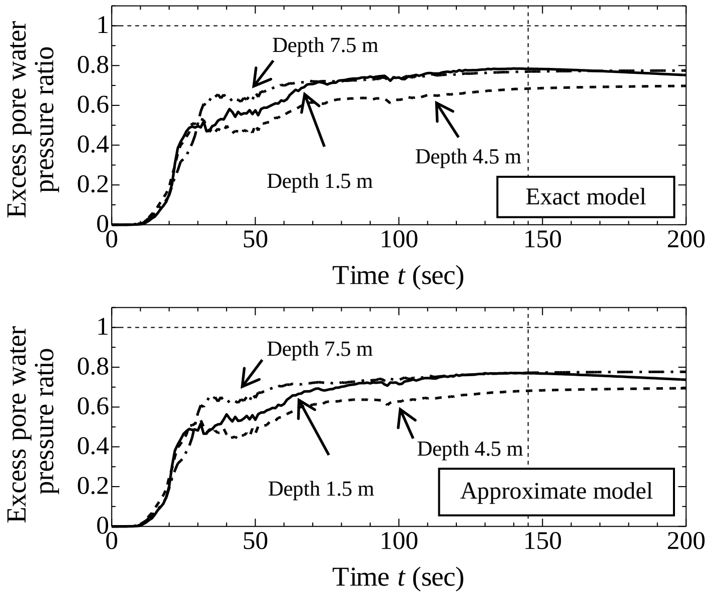

Unimproved

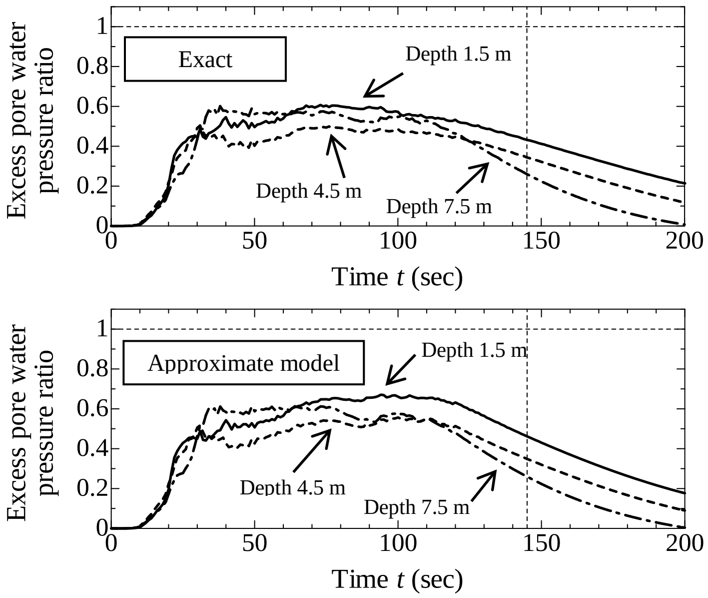

Improved (d = 0.9 m)

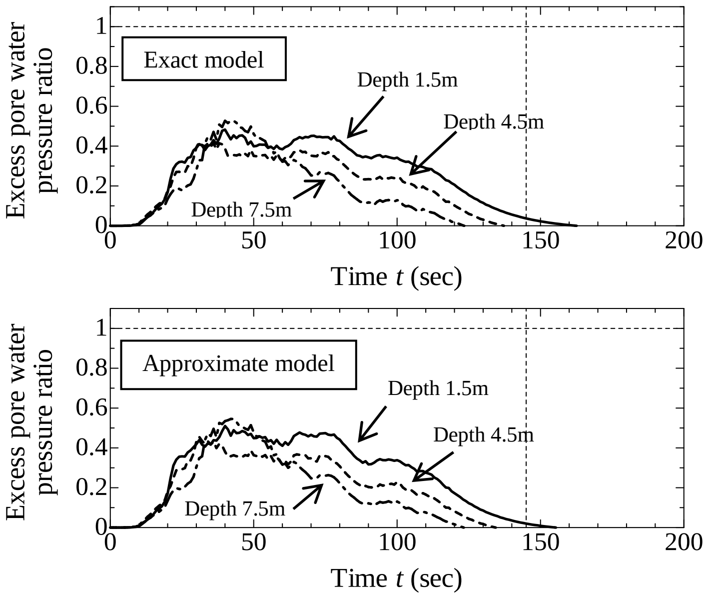

Improved (d = 0.6 m)

Fig. 7. Time-EPWP ratios.

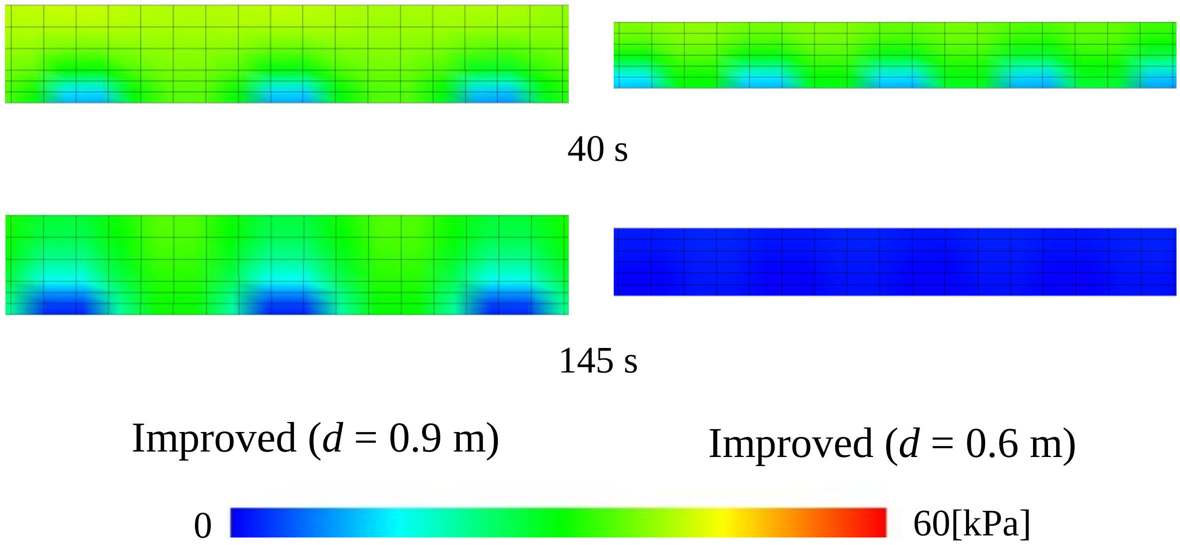

Fig. 8. Distributions of EPWP (*x*-*y* cross section, Depth 4.5 m).

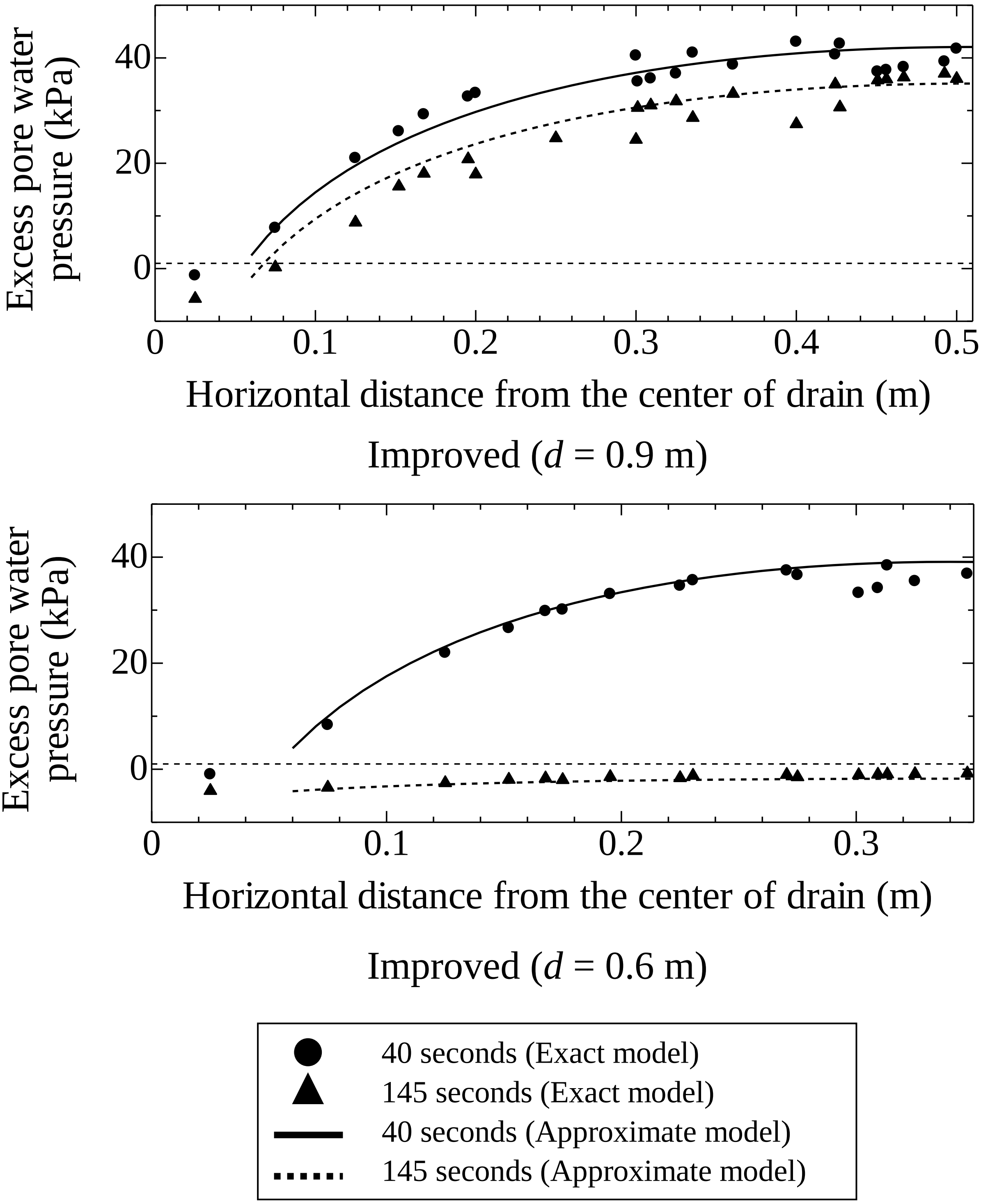

Fig. 9. EPWP along the distance from the center of drain.

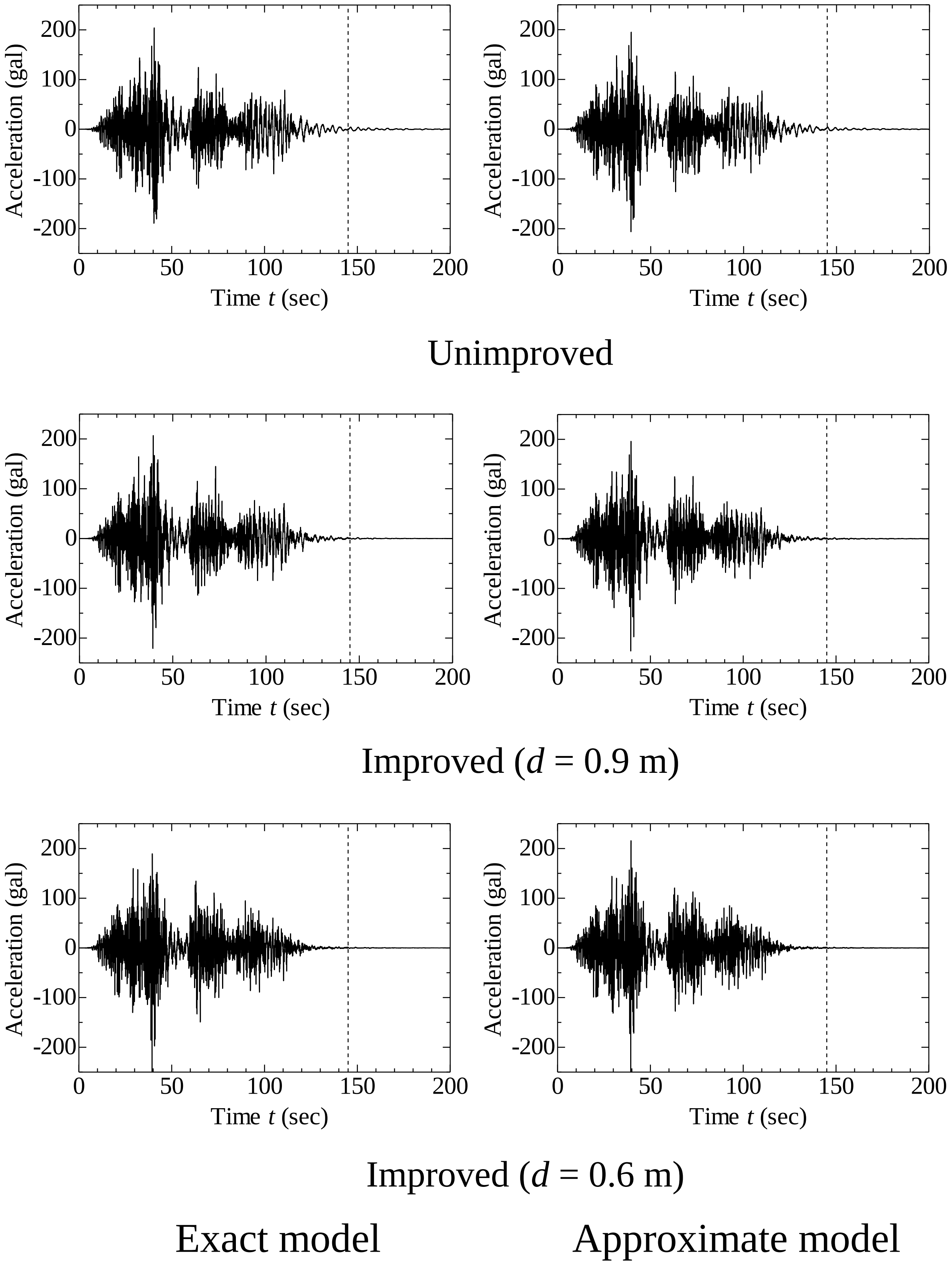

Fig. 10. Acceleration responses (x direction).

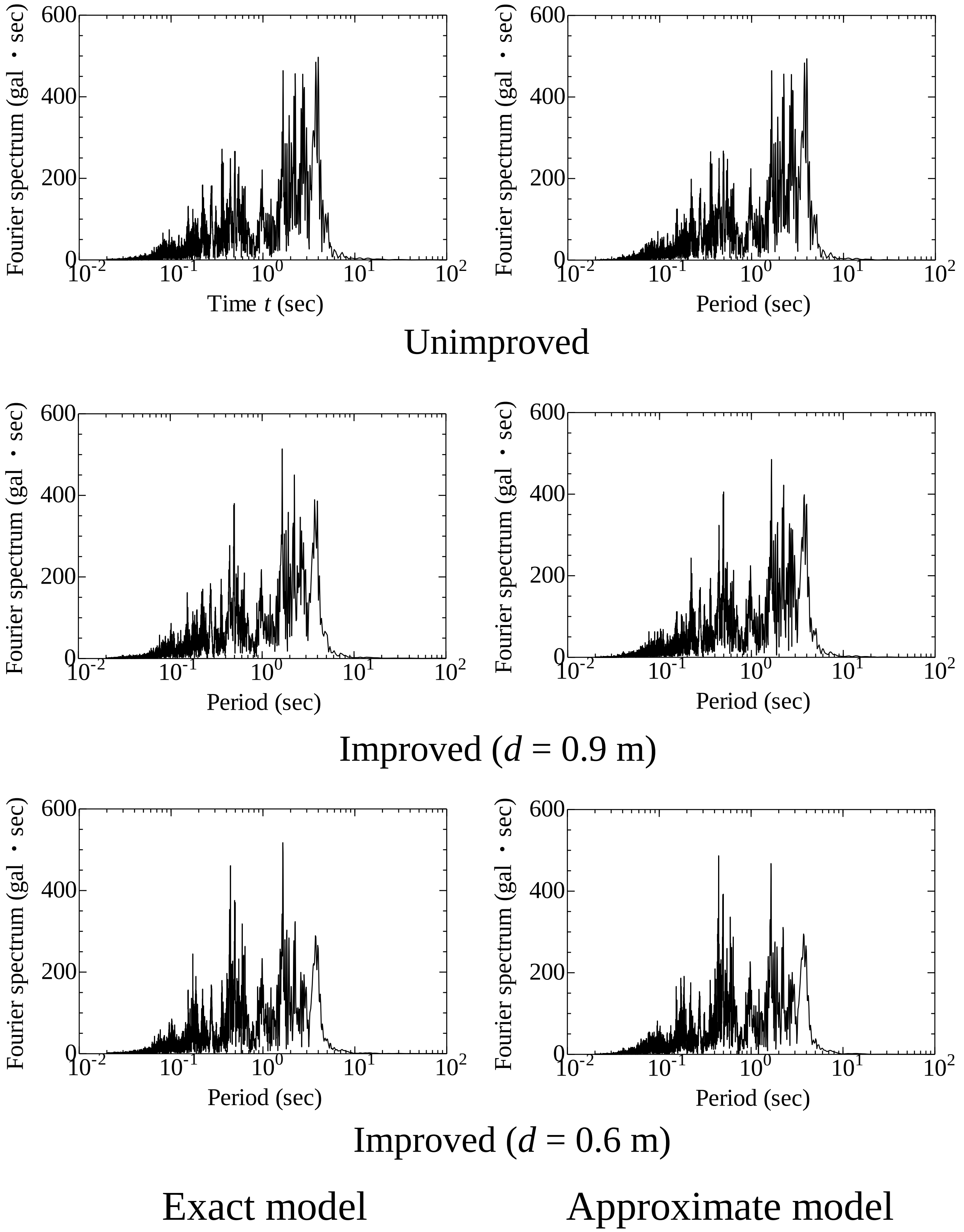

Fig. 11. Fourier spectrums of acceleration response (*x* direction).

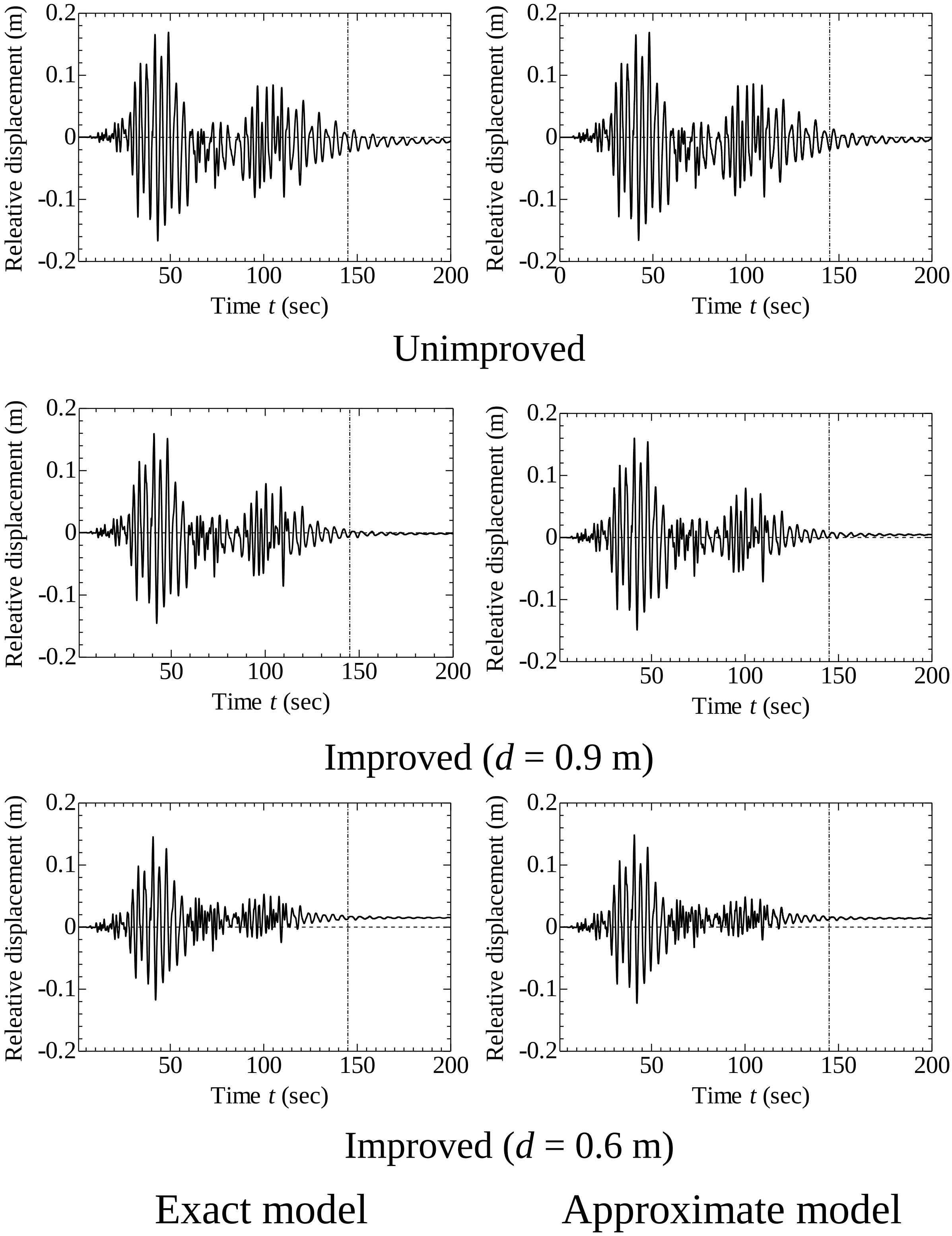

Fig. 12. Relative displacement responses (x direction).

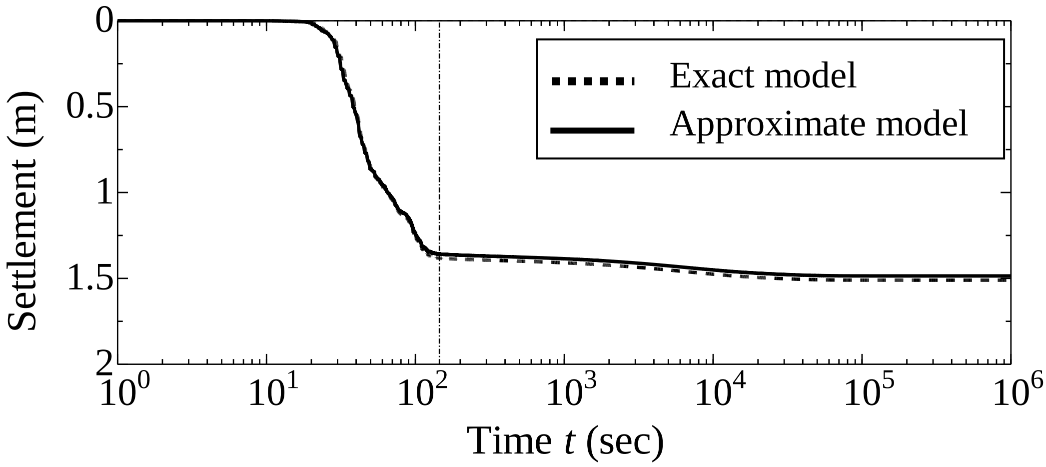

Unimproved

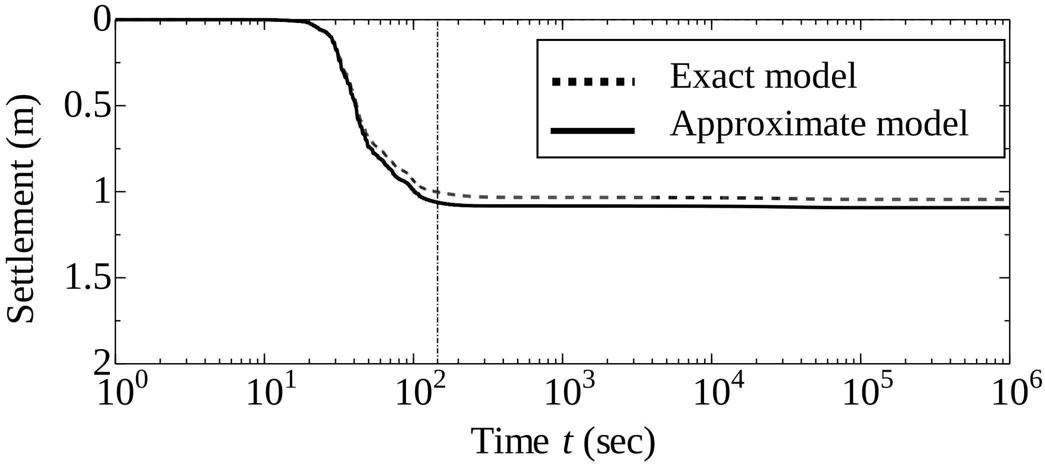

Improved (d = 0.9 m)

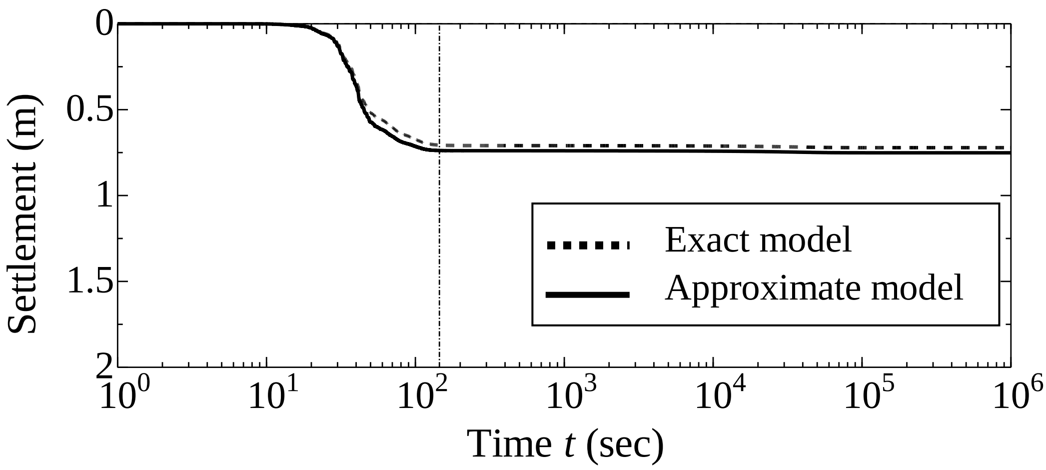

Improved (d = 0.6 m)

Fig. 13. Settlement behaviours.

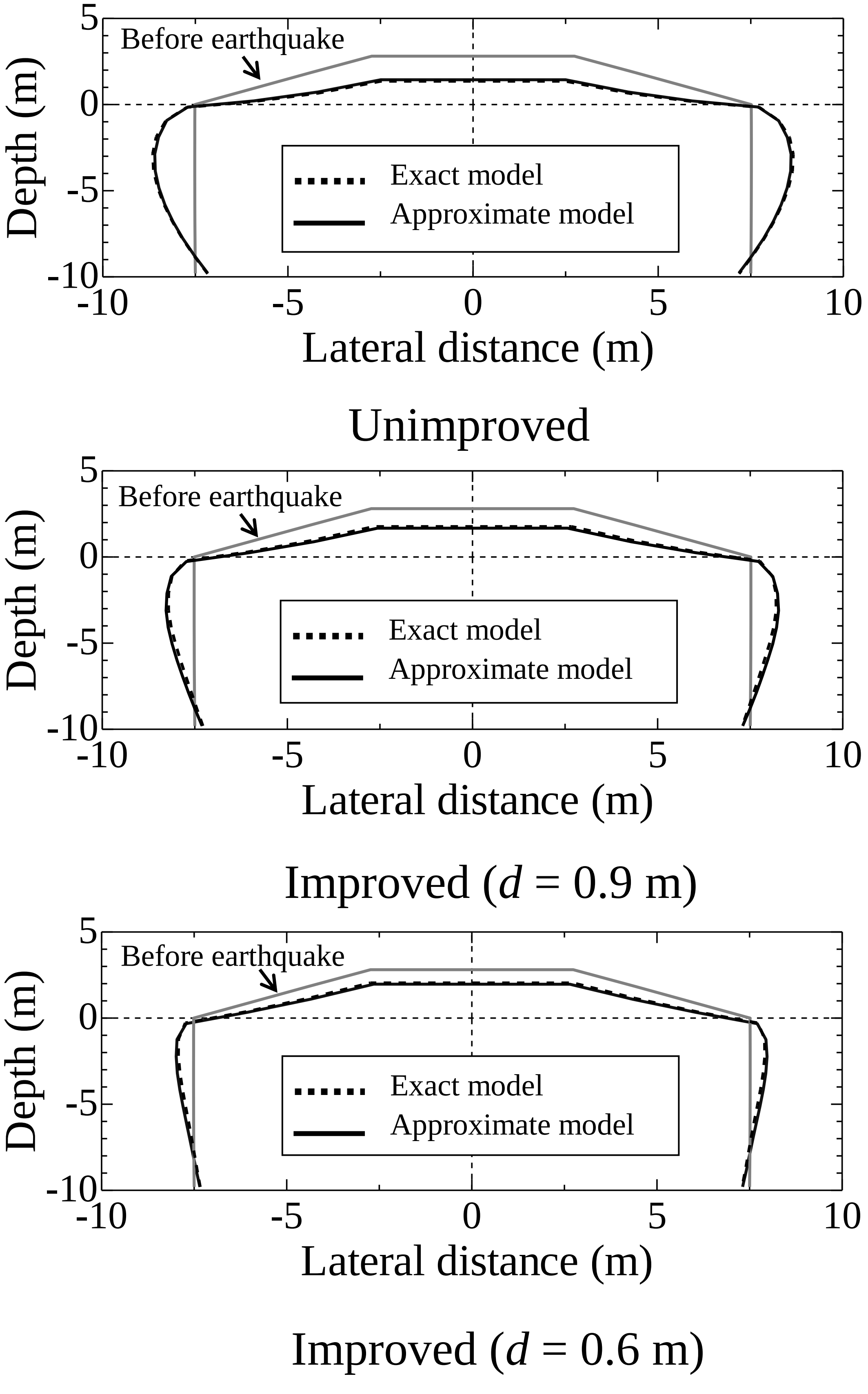

Fig. 14. Deformations of improved region and embankment.

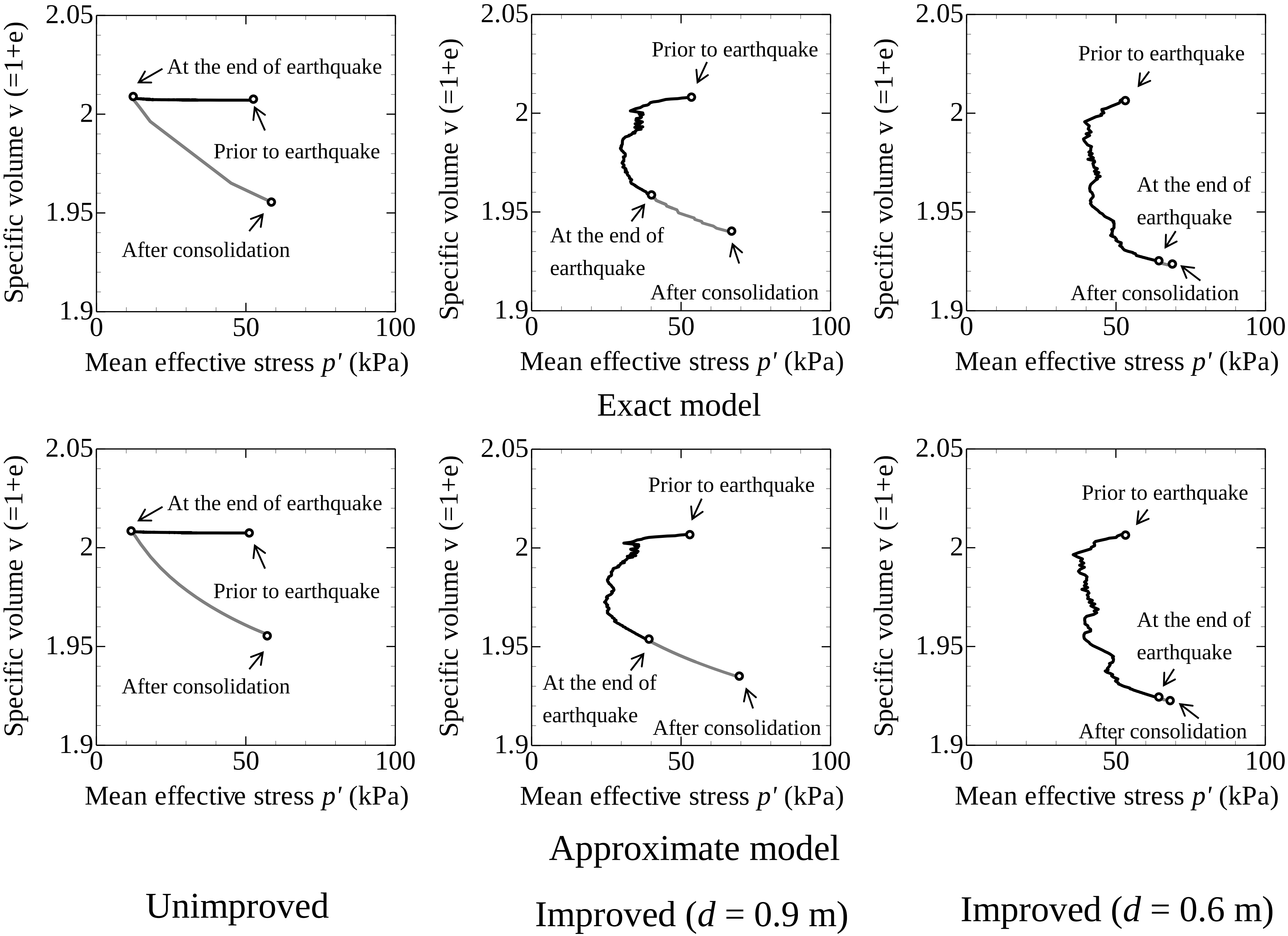

Fig. 15. Relationships between the mean effective stress and the specific volume.

Answer for Reviewers' comments.

1. GENERAL COMMENTS TO AUTHORS

After reviewing the revised manuscript, the editor has confirmed that the authors answered to the reviewers' comments and corrected properly. However there are still some items for which editorial revisions are required.

GENERAL COMMENTS TO EDITORS

We are grateful for the reviewers' comments and useful suggestions that have helped us to improve our manuscript. As described in the following responses, we have taken almost all the comments and suggestions into account in the revised manuscript. Please note that the revised sentences and equations are shown in blue in the revised manuscript.

2. REVISIONS

- *Items for which editorial revisions are required:*

E1. Page 11, Lines 238-240: In reply to the comment E3 for previous manuscript, the authors have rephrased the sentence. However, the reviewer still feels that the expression "… can be separated from …" in the revised sentence may confuse or mislead the readers. For example, "the mesh division can be specified independently of the drain arrangement …," as in Line 185, may be easier to read.

Answer (E1): Revised according to the comment.

E2. Page 20, Equations (A5) and (A6): The authors have revised the equation in reply to E8. However, the reviewer still doubts that the equation may be incorrect. Obviously, the second equation separated by comma in (A6) appears to be isolated from F(n). The reviewer has checked independently the derivation of Eqs. (A5) and (A6) using Eqs. (A2), (A3), and (A4), and thereby obtained:

Equation (A5): u^bar (z,t) = g(z,t) * F(n) + u_w(z,t), and

Equation (A6): F(n) = ln(n) - (3 n^2 - 2)/(4 n^2), n = r_e/r_w.

Please check again these equations carefully. This comment also applies to Eq. (5) in Section 2.

Answer (E2): We appreciate for your checking out our manuscript in detail. There was a typo in Eq. (A6), but Eq. (A5) is correct. The derivation of Eqs. (A5) and (A6) are shown below. Please note that the distribution of the approximated water pressure switches at $r = r_w$.

$$u(r,z,t) = \begin{cases} u_w(z,t) & (0 \le r < r_w) \\ g(z,t)f(r) + u_w(z,t) & (r_w \le r < r_e) \end{cases} \tag{A2}$$

$$f(r) = \ln\frac{r}{r_w} - \frac{r^2 - r_w^2}{2r_e^2} \tag{A3}$$

$$\bar{u}(z,t)=\frac{2\pi\int_0^{r_e}u(r,z,t)rdr}{\pi r_e^2} \tag{A4}$$

$$
\begin{aligned}
&=\frac{2}{r_e^2}\left\{\int_0^{r_w}u_w(z,t)rdr+\int_{r_w}^{r_e}\left(g(z,t)f(r)+u_w(z,t)\right)rdr\right\}\\
&=\frac{2}{r_e^2}\left(\int_{r_w}^{r_e}g(z,t)f(r)rdr+\int_0^{r_e}u_w(z,t)rdr\right)\\
&=\frac{2}{r_e^2}\left(g(z,t)\int_{r_w}^{r_e}f(r)rdr+u_w(z,t)\int_0^{r_e}rdr\right)\\
&=\frac{2}{r_e^2}\left(g(z,t)\frac{r_e^2}{2}F(n)\frac{n^2-1}{n^2}+u_w(z,t)\frac{r_e^2}{2}\right)
\end{aligned}
$$

$$=g(z,t)\frac{n^2-1}{n^2}F(n)+u_w(z,t) \tag{A5}$$

$$F(n)=\frac{n^2}{n^2-1}\ln n-\frac{3n^2-1}{4n^2},\quad n=\frac{r_e}{r_w} \tag{A6}$$

Eq. (5) and (A6) has been revised and Eq. (A2) has been rewritten to define the approximated water pressure more clearly.

E3. Line 181: A phrase "the element's stiffness" may be more suitable. Line 428: "by comparing with model experiments …" Line 314: Please delete unnecessary comma in "… away from drains, (both distance …"

Answer (E3): Revised according to the comment.